JOURNAL OF COMPUTATIONAL PHYSICS **129,** 233–242 (1996)
ARTICLE NO. 0246

A Technique for Embedding Clusters in Ionic Crystals Using the GAUSSIAN 92 Quantum Chemical Program

A. C. Lewandowski* and T. M. Wilson†

**Optex Communications Corporation, 2 Research Court, Rockville, Maryland 20850; †Computational Solid State Research Laboratory, Physics Department, Oklahoma State University, Stillwater, Oklahoma 74078*

Received February 23, 1996; revised July 5, 1996

We present a technique for embedding clusters of atoms, which are to be treated quantum mechanically, in ionic crystals by representing the external lattice by classical lattice-centered Gaussian charge distributions. The goal is to carry out *ab initio* self-consistent field calculations of the many-electron ground and excited states of finite clusters representing defects in an otherwise perfect crystal lattice. We describe a procedure for determining the effective charges and Gaussian exponents describing the external lattice so that, together with Hartree–Fock force calculations, the net forces on the quantum mechanical cluster ions are zero in the ground state. The result of this procedure is the production of an external coulombic field that has the same symmetry as the crystal, exactly balances the quantum mechanical forces, and simultaneously accounts for the fact that the external charge distribution is finite. The method is illustrated by considering the formation of the F-center defect in CaF_2.

I. INTRODUCTION

A crucial difference between isolated molecular and crystal defect electronic structure calculations rests in the treatment of the crystal field. For free-space calculations the forces on the atoms in a molecule are determined solely on the basis of their interactions with the other cluster atoms and, in the ground state the net forces on the atoms are zero. However, for a defect in a solid, the known geometry of a representative cluster generally would not correspond to the stable geometry for that cluster in free space. Another important distinction is that, for *ab initio* molecular calculations, the atoms in a cluster are typically treated at the same level of quantum chemical theory so that, for instance, the forces, geometry, and electronic structure of the entire system are determined solely on the basis of an approximate solution to the Schrödinger equation. However, depending on which properties one wishes to calculate and depending upon whether one can reasonably assume that these properties are described adequately by localized wave functions, then an alternative approach is to define regions of interest. For impurity/defect centers in ionic crystals which present themselves as deep, localized energy states within the band gap such a case appears to be operative. As such, one may introduce an approximation whereby excitations occurring within these centers are only weakly coupled to the nonlocalized conduction and valence band states. Within this approximation, no formal coupling is attempted, but instead, localized states are calculated quantum mechanically within the defect region under the influence of an effective coulombic field representing the surrounding host lattice.

In many areas of experimental spectroscopy there is a need to calculate the many-electron ground and excited states of impurity/defect centers in crystals. In many cases one wishes to obtain the energies of excited states which possess the same spatial and spin symmetry as the ground state. At present, the only generally applicable and feasible nonperturbative method for this is multiconfigurational complete active-space self-consistent field (CASSCF). This method is fully implemented in the GAUSSIAN 92 [1] quantum chemical program system. However, since GAUSSIAN 92 has its origins in quantum chemistry, it presently lacks a sophisticated embedding methodology. Thus, it is the purpose of this article to present an embedding procedure that can be implemented within the context of the GAUSSIAN 92 program system and thus within the context of being able to perform follow-on CASSCF calculations. Toward this end, we develop an approximate cluster embedding methodology exploiting a key feature in GAUSSIAN 92 which permits the inclusion into the Fock operator terms reflecting a distribution of either external point ions or external Gaussian charge distributions. This capability allows for Hartree–Fock SCF, configuration interaction, and CASSCF calculations on a quantum cluster in the presence of an external arrangement of charge which is used to represent a perfect crystal lattice [2, 3]. Also provided is an option to calculate forces on the cluster nuclei which arise from interactions with other cluster nuclei and the overall cluster electronic charge density suitably perturbed by the presence of an external charge distribution.

For this technique we define two regions of interest, namely, the quantum cluster and, an external charge distri-

0021-9991/96 $18.00

bution. The quantum cluster consists of that portion of the perfect crystal that is to be treated quantum mechanically and will ultimately contain the defect. The external ions are treated classically and are represented by lattice-centered Gaussians of the form $q_i(\alpha_i/\pi)^{3/2}\exp(-\alpha_i|\mathbf{r}\text{-}\mathbf{R}_i^{\mathrm{ex}}|^2)$. The parameters q_i and α_i, represent the overall charge and Gaussian exponent respectively of an external ion at $\mathbf{R}_i^{\mathrm{ex}}$. In developing an embedding scheme one must have a known point of reference in order to ascertain when the embedding process is complete. Since the equilibrium geometry of the nondefective cluster is known, we have chosen to establish an external charge distribution such that the net forces on the cluster ions are zero. To achieve this, the parameters q_i and α_i, are adjusted in conjunction with Hartree–Fock force calculations to stabilize the cluster in the ground state. The interactions within the external charge distribution contribute to the overall energy of the system and are treated classically. By the end of the embedding procedure, an effective external coulombic field is produced in the quantum cluster region that has the same symmetry as the crystal, exactly balances the quantum mechanical forces on the cluster ions, and simultaneously accounts for the fact that the external charge distribution is finite.

To illustrate this method we consider the formation of the F-center defect in CaF_2. It should be noted that while the following iterative embedding scheme will be performed at the Hartree–Fock level of theory, in principle SCF force calculations based on correlated methods such as CI singles and doubles (CISD) or CASSCF are possible.

We note that other lattice-embedded electronic structure programs have evolved over the last decade. Perhaps the most advanced is the ICECAP program system [4]. ICECAP possesses a sophisticated cluster embedding technology based on the Kunz–Klein localizing potential [5] and the classical shell model for the external lattice [6] and has been applied to a variety of systems [7, 8]. Presently, however, ICECAP lacks the CASSCF capability. Thus, within the ICECAP program system, states other than the ground state can only be analyzed by applying symmetry constraints to the calculation.

Finally, mention should also be made of some recent work on the embedding problem by Winter, Pitzer, and Temple [9] and Martin and Hay [10]. The external lattice is modeled by placing l-dependent effective core potentials on some or all of the ions external to the quantum cluster. These potentials are determined by fitting to a linear combination of Gaussians the core potentials obtained from numerical Hartree–Fock calculations of the free atom. This method has achieved a certain degree of success in predicting the geometry for the NaF:Cu system. However this method, unlike ICECAP and the technique presented in this article, does not iterate between SCF cluster calculations and external lattice parameter adjustments to either minimize the energy (as with ICECAP), or minimize the cluster forces at the experimental geometry (as with our method).

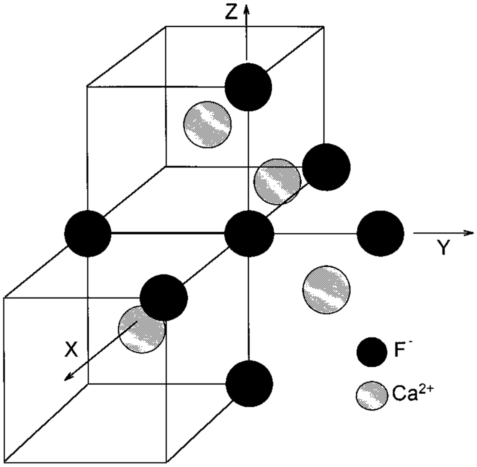

FIG. 1. Diagram of the nondefective cluster, $(Ca_4F_7)^{+1}$. The ions are arranged at the experimental Ca-F distance of 2.3656 Å [11]. SCF calculations based on this cluster are used to determine the embedding lattice parameters.

II. CLUSTER EMBEDDING

A. *Overview of the Method*

We start with the nondefective cluster shown in Fig. 1. This figure shows the $(Ca_4F_7)^{1+}$ cluster that will be treated quantum mechanically and serves to define the coordinate system. The ions are arranged at the experimental Ca-F distance of 2.366 Å [11]. After embedding, the F-center defect will be formed from this cluster by the removal of the central F^- ion to form a vacancy, the addition of an electron, and geometry relaxation. Referring to the flowchart in Fig. 2, the embedding method consists of the following stages.

(1) Construct the nondefective quantum cluster. This cluster is the portion of the perfect crystal that is to be treated quantum mechanically and will ultimately contain the defect. The geometry of this cluster is chosen to be that of the perfect crystal as known experimentally. Optimize the basis set, choose the CASSCF active spaces.

(2) Perform an SCF calculation for the cluster in isolation to determine the forces on the cluster ions $\mathbf{F}^{(0)}_{\mathrm{clus}}(\mathbf{R}_j)$. The force calculated on each cluster ion is the result of its electrostatic interaction with the other cluster nuclei and with the cluster SCF electronic charge density.

(3) Construct around this cluster a point ion field consisting of representative point charges for the ions in the crystal. These external point charges are assigned the va-

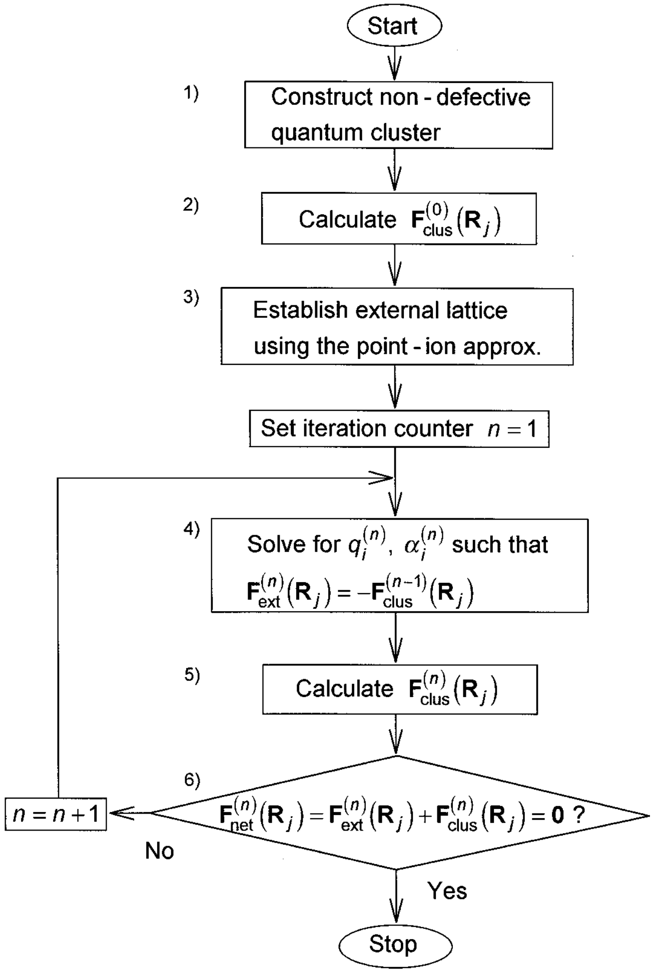

FIG. 2. Flowchart showing the series of steps involved in embedding a nondefective quantum cluster in an external arrangement of Gaussian charge distributions. The symbols are defined in the text.

lence charges of the ions comprising the crystal (for instance, +2 for Ca and −1 for F in CaF_2) and arranged in the host lattice structure. The size of this external arrangement is chosen so as to produce as close as possible the cluster-subtracted Madelung potentials at the quantum cluster nuclear sites. The cluster-subtracted Madelung potentials are obtained by subtracting from the Madelung potentials those contributions arising from the other ions comprising the quantum cluster.

(4) Allow the external point ions to take on an extension in the form of a Gaussian distribution of the charge centered about each external lattice site. By adjusting the charges, $q_i^{(n)}$, and the Gaussian exponents, $\alpha_i^{(n)}$, on these sites the external charge distribution can be determined so that the external electrostatic forces, $\mathbf{F}^{(n)}_{\text{ext}}(\mathbf{R}_j)$, applied to the cluster nuclei exactly balance the SCF cluster forces previously calculated.

(5) Using the charges and Gaussian exponents determined in the previous step, perform another SCF force calculation to determine the new cluster forces $\mathbf{F}^{(n)}_{\text{clus}}(\mathbf{R}_j)$. These new SCF forces will be different from the previous SCF cluster forces since the SCF density must now react to the presence of the new external charge distribution. While the SCF density does reflect the presence of the external arrangement of charge, the force on a particular cluster ion calculated by GAUSSIAN 92 does not include the direct coulombic interactions between the cluster nucleus and the external lattice. Presently, these interactions must be included separately.

(6) The net force on the cluster nuclei, $\mathbf{F}^{(n)}_{\text{net}}(\mathbf{R}_j)$, is $\mathbf{F}^{(n)}_{\text{ext}}(\mathbf{R}_j) + \mathbf{F}^{(n)}_{\text{clus}}(\mathbf{R}_j)$. If the net forces are not negligible then increment the iteration counter and determine new Gaussian lattice parameters to balance the SCF cluster forces. This process of SCF force calculations and external charge variation is continued until convergence is achieved. When the net forces on the cluster nuclei become negligible the embedding procedure is complete. Note that during this entire process the geometry of the nondefective cluster is maintained at the experimentally known perfect crystal geometry. At the end of this process one is left with a system consisting of a nondefective quantum cluster and an external lattice-centered Gaussian charge distribution such that the forces calculated quantum mechanically within the cluster are exactly balanced by the forces exerted electrostatically by the external charge.

With the embedding operation complete, the defect is formed within the quantum cluster. For these calculations, this is done by removing the central F^- ion to form a vacancy. With the external field parameters unchanged, the defective quantum cluster is geometry-optimized. Finally, the ground and excited states and other properties of interest are calculated by the method of CASSCF.

The method outlined above is a force minimization scheme. While it is more common in quantum chemistry to follow energy minimization schemes, the energy equations for this particular lattice embedding problem do not as easily lend themselves to a simple and straightforward iterative procedure. We note that this method is nonperturbative. Since the external charge source terms enter into the Fock operator, the SCF procedure generates an antisymmetric wave function that is fully distorted by the external field. Thus, the only approximations that enter into the embedding procedure (other than the approximations inherent in the SCF procedure itself) stem from the nature and composition of the external arrangements.

B. *Mathematical Development*

We begin the mathematical development by considering an external charge density $\rho_{\text{ext}}(\mathbf{r})$ which produces an external electrostatic potential $V_{\text{ext}}(\mathbf{r})$. From classical electrostatics, the external potential is given by

$$V_{\text{ext}}(\mathbf{r}) = \int \frac{\rho_{\text{ext}}(\mathbf{r}')}{|\mathbf{r} - \mathbf{r}'|} d\mathbf{r}'. \tag{1}$$

If we assume that the external charge density is described by an arrangement of lattice-centered Gaussians [2, 3] then

$$\rho_{\text{ext}}(\mathbf{r}) = \sum_{i=1}^{N} q_i \left(\frac{\alpha_i}{\pi}\right)^{3/2} e^{-\alpha_i|\mathbf{r}-\mathbf{R}_i^{\text{ex}}|^2}, \tag{2}$$

where N is the number of external lattice sites, $\mathbf{R}_i^{\text{ex}}$ locates the external lattice sites, q_i is the total charge associated with lattice site i, and α_i is the Gaussian exponent associated with lattice site i. Substituting Eq. (2) into Eq. (1), integration produces

$$V_{\text{ext}}(\mathbf{r}) = \sum_{i=1}^{N} q_i \frac{\operatorname{erf}[\sqrt{\alpha_i}|\mathbf{R}_i^{\text{ex}} - \mathbf{r}|]}{|\mathbf{R}_i^{\text{ex}} - \mathbf{r}|}, \tag{3}$$

where the error function is defined

$$\operatorname{erf}(x) = \frac{2}{\sqrt{\pi}} \int_0^x e^{-u^2} du. \tag{4}$$

The quantum cluster electronic charge density, $\rho_{\text{clus}}(\mathbf{r})$, is obtained from a Hartree–Fock SCF calculation and is given by [12]

$$\rho_{\text{clus}}(\mathbf{r}) = \sum_{\nu=1}^{K} \sum_{\mu=1}^{K} P_{\nu\mu} \phi_\nu(\mathbf{r}) \phi_\mu(\mathbf{r}), \tag{5}$$

where K is the number of basis functions, $P_{\nu\mu}$ is the density matrix, and $\phi_\nu(\mathbf{r})$ and $\phi_\mu(\mathbf{r})$ are the primitive Gaussian basis functions of type ν and μ centered on cluster sites $\mathbf{R}_\nu$ and $\mathbf{R}_\mu$. The internal quantum cluster potential $V_{\text{clus}}(\mathbf{r})$ is then

$$V_{\text{clus}}(\mathbf{r}) = \sum_{\nu=1}^{K} \sum_{\mu=1}^{K} P_{\nu\mu} \int \frac{\phi_\nu(\mathbf{r}')\phi_\mu(\mathbf{r}')}{|\mathbf{r} - \mathbf{r}'|} d\mathbf{r}', \tag{6}$$

and the potential due to the atomic nuclei in the cluster is

$$V_{\text{core}}(\mathbf{r}) = \sum_{i=1}^{M} \frac{Z_i}{|\mathbf{r} - \mathbf{R}_i|}, \tag{7}$$

where M is the number of nuclei in the cluster and Z_i is the nuclear charge on cluster nucleus i at site $\mathbf{R}_i$. With the total electrostatic field $\mathbf{E}(\mathbf{r})$ written as

$$\mathbf{E}(\mathbf{r}) = -\nabla V_{\text{clus}}(\mathbf{r}) - \nabla V_{\text{core}}(\mathbf{r}) - \nabla V_{\text{ext}}(\mathbf{r}), \tag{8}$$

we have

$$\begin{aligned}\mathbf{E}(\mathbf{r}) = {} & \sum_{\nu=1}^{K} \sum_{\mu=1}^{K} P_{\nu\mu} \int \frac{\phi_\nu(\mathbf{r}')\phi_\mu(\mathbf{r}')}{|\mathbf{r} - \mathbf{r}'|^3} (\mathbf{r} - \mathbf{r}') d\mathbf{r}' \\ & + \sum_{i=1}^{M} Z_i \frac{\mathbf{r} - \mathbf{R}_i}{|\mathbf{r} - \mathbf{R}_i|^3} - \sum_{i=1}^{N} q_i \nabla \frac{\operatorname{erf}[\sqrt{\alpha_i}|\mathbf{R}_i^{\text{ex}} - \mathbf{r}|]}{|\mathbf{R}_i^{\text{ex}} - \mathbf{r}|}.\end{aligned} \tag{9}$$

The first two terms in Eq. (9) contain information concerning the cluster only, therefore, define these first two terms to be $\mathbf{E}_{\text{clus}}(\mathbf{r})$, that is, the total field due to the quantum mechanical electronic density and the nuclear charges. By evaluating Eq. (9) at one of the quantum cluster nuclear sites, say $\mathbf{R}_j$, then the symmetry of the cluster and surrounding lattice will allow considerable simplification of the field and force equations. Let $\mathbf{E}'_{\text{clus}}(\mathbf{R}_j)$ represent the internal cluster field evaluated at $\mathbf{R}_j$ with the nuclear core at $\mathbf{R}_j$ excluded from the sum over the nuclei. If the origin is located on the central cluster ion as shown in Fig. 1 then, by symmetry, the total electric field vector must at most have only a radial component. Therefore, the $\hat{\theta}$ and $\hat{\phi}$ components of the ∇ operator must vanish by symmetry when evaluated at $\mathbf{R}_j$. We then have

$$\begin{aligned}\nabla \frac{\operatorname{erf}[\sqrt{\alpha_i}|\mathbf{R}_i^{\text{ex}} - \mathbf{r}|]}{|\mathbf{R}_i^{\text{ex}} - \mathbf{r}|}\Bigg|_{\mathbf{r}=\mathbf{R}_j} &= \left(\frac{R_j - \mathbf{R}_j \cdot \mathbf{R}_i^{\text{ex}}/R_j}{|\mathbf{R}_i^{\text{ex}} - \mathbf{R}_j|^2}\right) \\ & \left(2\sqrt{\frac{\alpha_i}{\pi}} \exp[-\alpha_i|\mathbf{R}_i^{\text{ex}} - \mathbf{R}_j|^2] - \frac{\operatorname{erf}[\sqrt{\alpha_i}|\mathbf{R}_i^{\text{ex}} - \mathbf{R}_j|]}{|\mathbf{R}_i^{\text{ex}} - \mathbf{R}_j|}\right)\hat{\mathbf{r}} \\ & \equiv \mathbf{I}_i(\mathbf{R}_j).\end{aligned} \tag{10}$$

Equation (9) then becomes

$$\mathbf{E}(\mathbf{R}_j) = \mathbf{E}'_{\text{clus}}(\mathbf{R}_j) - \sum_{i=1}^{N} q_i \mathbf{I}_i(\mathbf{R}_j). \tag{11}$$

For CaF_2 we will choose to represent the external charge distribution by two different types of lattice-centered Gaussians characterized by different charges and Gaussian exponents $(q_{\text{F}}, \alpha_{\text{F}})$ and $(q_{\text{Ca}}, \alpha_{\text{Ca}})$. Since, in principle, the nondefective cluster in the ground state should not polarize the surrounding lattice, one should be able to approximate the external lattice by only "F-type" and "Ca-type" lattice-centered Gaussians. This done, Eq. (11) becomes

$$\mathbf{E}(\mathbf{R}_j) = \mathbf{E}'_{\text{clus}}(\mathbf{R}_j) - q_{\text{F}} \sum_{i=1}^{N_{\text{F}}} \mathbf{I}_i^{\text{F}}(\mathbf{R}_j) - q_{\text{Ca}} \sum_{i=1}^{N_{\text{Ca}}} \mathbf{I}_i^{\text{Ca}}(\mathbf{R}_j), \tag{12}$$

where N_{F} and N_{Ca} are the number F-type and Ca-type external lattice-centered Gaussians respectively. $\mathbf{I}_i^{\text{F}}(\mathbf{R}_j)$ is given by Eq. (10) with $\mathbf{R}_i^{\text{ex}}$ replaced by $\mathbf{R}_i^{\text{F}}$ and α_i replaced by α_{F} and similarly for $\mathbf{I}_i^{\mathrm{Ca}}(\mathbf{R}_j)$, $\mathbf{R}_i^{\mathrm{ex}}$ is replaced by $\mathbf{R}_i^{\mathrm{Ca}}$ and α_i by α_{Ca}.

Defining the vector functions,

$$\mathbf{K}_{\mathrm{F}}(\mathbf{R}_j) = \sum_{i=1}^{N_{\mathrm{F}}} \mathbf{I}_i^{\mathrm{F}}(\mathbf{R}_j), \quad \mathbf{K}_{\mathrm{Ca}}(\mathbf{R}_j) = \sum_{i=1}^{N_{\mathrm{Ca}}} \mathbf{I}_i^{\mathrm{Ca}}(\mathbf{R}_j), \qquad (13)$$

the total force on a nucleus with nuclear charge Z_j at site $\mathbf{R}_j$ in the quantum cluster is given by

$$\mathbf{F}(\mathbf{R}_j) = \mathbf{F}_{\mathrm{clus}}(\mathbf{R}_j) - Z_j q_{\mathrm{F}} \mathbf{K}_{\mathrm{F}}(\mathbf{R}_j) - Z_j q_{\mathrm{Ca}} \mathbf{K}_{\mathrm{Ca}}(\mathbf{R}_j). \qquad (14)$$

$\mathbf{F}_{\mathrm{clus}}(\mathbf{R}_j)$ is the force on the nucleus at site j due to interactions with the electronic charge density and the other nuclei within the cluster and is calculated by the GAUSSIAN 92 program. The terms involving the $\mathbf{K}(\mathbf{R}_j)$ functions represent the force on the nucleus at site j due to interactions with the external charge distribution.

When the cluster is completely stabilized, $\mathbf{F}(\mathbf{R}_j) = \mathbf{0}$. Also since $\mathbf{F}_{\mathrm{clus}}(\mathbf{R}_j)$, $\mathbf{K}_{\mathrm{F}}(\mathbf{R}_j)$, and $\mathbf{K}_{\mathrm{Ca}}(\mathbf{R}_j)$ only have components along the $\hat{\mathbf{r}}$-direction (as defined in Fig. 1), we may write Eq. (14) for the stable cluster as a scalar equation. Thus,

$$F_{\mathrm{clus}}(\mathbf{R}_j) = Z_j q_{\mathrm{F}} K_{\mathrm{F}}(\mathbf{R}_j) + Z_j q_{\mathrm{Ca}} K_{\mathrm{Ca}}(\mathbf{R}_j), \qquad (15)$$

where it is understood that positive (negative) forces indicate that the vector is directed outward (inward) along the $\hat{\mathbf{r}}$-direction. Defining the scalar functions,

$$\begin{aligned} J_{\mathrm{F}}(\mathbf{R}_j) &= \sum_{i=1}^{N_{\mathrm{F}}} \frac{\mathrm{erf}[\sqrt{\alpha_{\mathrm{F}}}|\mathbf{R}_i^{\mathrm{F}} - \mathbf{R}_j|]}{|\mathbf{R}_i^{\mathrm{F}} - \mathbf{R}_j|}, \\ J_{\mathrm{Ca}}(\mathbf{R}_j) &= \sum_{i=1}^{N_{\mathrm{Ca}}} \frac{\mathrm{erf}[\sqrt{\alpha_{\mathrm{Ca}}}|\mathbf{R}_i^{\mathrm{Ca}} - \mathbf{R}_j|]}{|\mathbf{R}_i^{\mathrm{Ca}} - \mathbf{R}_j|}, \end{aligned} \qquad (16)$$

the electrostatic potential due to the external arrangement of F-type and Ca-type lattice-centered Gaussians is simply

$$V_{\mathrm{ext}}(\mathbf{R}_j) = q_{\mathrm{F}} J_{\mathrm{F}}(\mathbf{R}_j) + q_{\mathrm{Ca}} J_{\mathrm{Ca}}(\mathbf{R}_j). \qquad (17)$$

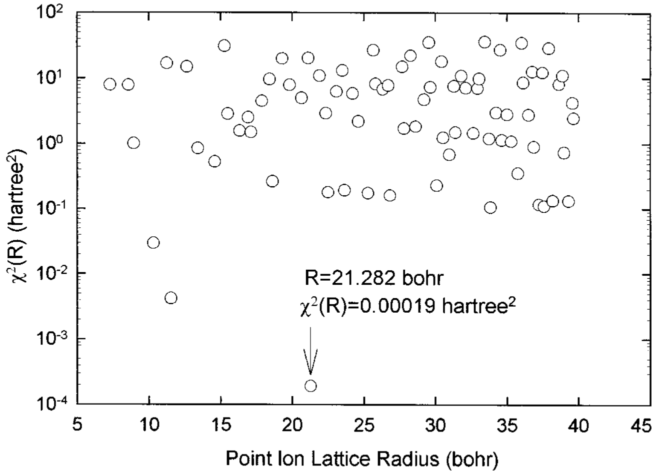

FIG. 3. Plot of $\chi^2(R_{\mathrm{ext}}^{\mathrm{pi}})$ vs $R_{\mathrm{ext}}^{\mathrm{pi}}$ for the distribution of point ions arranged outside the cluster in the $\mathrm{CaF_2}$ lattice structure with -1 point ions corresponding to F-sites and $+2$ point ions corresponding to Ca-sites. Over this range, the lowest $\chi^2(R_{\mathrm{ext}}^{\mathrm{pi}})$ occurs for $R_{\mathrm{ext}}^{\mathrm{pi}} = 21.282$ bohr.

C. *Choosing the External Lattice Size*

Equations (15) and (17) form the mathematical basis for the application of this method. Before this is done the first step will be to choose the size of the external arrangement of lattice-centered Gaussians. The nondefective cluster shown in Fig. 1 contains four symmetry distinct sites: (1) the central F^- site at $\mathbf{R}_{\mathrm{F0}}$, (2) an outer F^- site at $\mathbf{R}_{\mathrm{F}}$, (3) a Ca^{+2} site at $\mathbf{R}_{\mathrm{Ca}}$, and (4) the interstitial site at $\mathbf{R}_{\mathrm{int}}$. As a consequence, it is only necessary to solve Eqs. (15) and (17) at these sites and then by symmetry they are automatically satisfied at the other sites reachable by a symmetry operation. The Madelung potentials at these sites are given in the literature [11]. After subtracting the contribution to the Madelung potentials at these sites due to the presence of the quantum cluster ions, the cluster-subtracted Madelung potentials are: $\phi(\mathbf{R}_{\mathrm{F0}}, \infty) = -0.2328$ hartree, $\phi(\mathbf{R}_{\mathrm{F}}, \infty) = -0.1292$ hartree, $\phi(\mathbf{R}_{\mathrm{Ca}}, \infty) = -0.3099$ hartree, and $\phi(\mathbf{R}_{\mathrm{int}}, \infty) = -0.1965$ hartree. The criterion used to determine the best external lattice size will be to choose a finite radius $R_{\mathrm{ext}}^{\mathrm{pi}}$ of an external point ion lattice such that the electrostatic potential at the four symmetry-distinct cluster sites best approximates the cluster-subtracted Madelung potentials. That is, one wishes to minimize the function $\chi^2(R_{\mathrm{ext}}^{\mathrm{pi}})$ given by

$$\begin{aligned} \chi^2(R_{\mathrm{ext}}^{\mathrm{pi}}) = {} & (\phi(\mathbf{R}_{\mathrm{F0}}, \infty) - \phi(\mathbf{R}_{\mathrm{F0}}, R_{\mathrm{ext}}^{\mathrm{pi}}))^2 \\ & + (\phi(\mathbf{R}_{\mathrm{F}}, \infty) - \phi(\mathbf{R}_{\mathrm{F}}, R_{\mathrm{ext}}^{\mathrm{pi}}))^2 \\ & + (\phi(\mathbf{R}_{\mathrm{Ca}}, \infty) - \phi(\mathbf{R}_{\mathrm{Ca}}, R_{\mathrm{ext}}^{\mathrm{pi}}))^2 \\ & + (\phi(\mathbf{R}_{\mathrm{int}}, \infty) - \phi(\mathbf{R}_{\mathrm{int}}, R_{\mathrm{ext}}^{\mathrm{pi}}))^2, \end{aligned} \qquad (18)$$

where, for instance, $\phi(\mathbf{R}_{\mathrm{F}}, R_{\mathrm{ext}}^{\mathrm{pi}})$ is the potential at the cluster site $\mathbf{R}_{\mathrm{F}}$ due to an external $\mathrm{CaF_2}$ lattice of -1 and $+2$ point ions out to a radius $R_{\mathrm{ext}}^{\mathrm{pi}}$ excluding the cluster ions.

While it is obvious that $\chi^2(\infty)$ is the absolute minimum, local minima may be found for finite values of $R_{\mathrm{ext}}^{\mathrm{pi}}$ as shown in Fig. 3. This figure shows $\chi^2(R_{\mathrm{ext}}^{\mathrm{pi}})$ as a function of point ion shell radius $R_{\mathrm{ext}}^{\mathrm{pi}}$ out to a maximum of 40 bohr encompassing 2876 point ions (excluding the cluster ions). From this figure we see that over this range the minimum error occurs at $R_{\mathrm{ext}}^{\mathrm{pi}} = 21.282$ bohr. Excluding the cluster ions, this lattice consists of 298 sites of -1 charge (F-sites) and 148 sites of + 2 charge (Ca-sites) point ions. Kunz

TABLE I

Values of the Cluster-Subtracted Madelung Potentials $\phi(\mathbf{R}_j, \infty)$ and the External Point Ion Potentials $\phi(\mathbf{R}_j, R_{\text{ext}}^{\text{pi}})$, at Four Symmetry Distinct Sites, $\mathbf{R}_j$, within the Nondefective Cluster $(\text{Ca}_4\text{F}_7)^{+1}$

$\mathbf{R}_j$	$\phi(\mathbf{R}_j, \infty)$ (hartree)[a]	$\phi(\mathbf{R}_j, R_{\text{ext}}^{\text{pi}})$ (hartree)
F_0-site	−0.2328	−0.2397
F-site	−0.1292	−0.1357
Ca-site	−0.3099	−0.3188
Interstitial-site	−0.1965	−0.2011

Note. The external point ion distribution extends out to a radius of $R_{\text{ext}}^{\text{pi}} = 21.282$ bohr and produces a χ^2 $(R_{\text{ext}}^{\text{pi}})$ value of 0.00019 hartree^2.

[a] Calculated from data provided in Ref. [11].

and Vail [5] point out that the total charge (cluster + external ions) should be neutral to avoid a "spurious tunneling effect." In this case the total charge is −1 which is as small as could be obtained and still preserve the crystal symmetry. Table I shows the cluster-subtracted Madelung potentials at the four symmetry distinct sites and the external potential at these sites produced by the point ion lattice with $R_{\text{ext}}^{\text{pi}} = 21.282$ bohr.

D. *The Force Equations*

With size of the external distribution chosen using the point ion model, point ions are replaced by lattice-centered Gaussians and then Eqs. (15) and (17) are solved for the parameters $q_{\text{F}}, \alpha_{\text{F}}, q_{\text{Ca}}, \alpha_{\text{Ca}}$. With V_0 taken to be the cluster-subtracted Madelung potential at the central F^- site, the following equations can be solved,

$$Z_{\text{F}} q_{\text{F}} K_{\text{FF}} + Z_{\text{F}} q_{\text{Ca}} K_{\text{CaF}} = F_{\text{F}}, \tag{19}$$

$$Z_{\text{Ca}} q_{\text{F}} K_{\text{FCa}} + Z_{\text{Ca}} q_{\text{Ca}} K_{\text{CaCa}} = F_{\text{Ca}}, \tag{20}$$

$$q_{\text{F}} J_{\text{F0}} + q_{\text{Ca}} J_{\text{Ca0}} = V_0, \tag{21}$$

$$q_{\text{Ca}} = -2 q_{\text{F}}, \tag{22}$$

where $K_{\text{FF}} = K_{\text{F}}(\mathbf{R}_{\text{F}})$, $K_{\text{CaF}} = K_{\text{Ca}}(\mathbf{R}_{\text{F}})$, $K_{\text{FCa}} = K_{\text{F}}(\mathbf{R}_{\text{Ca}})$, $K_{\text{CaCa}} = K_{\text{Ca}}(\mathbf{R}_{\text{Ca}})$, $J_{\text{F0}} = J_{\text{F}}(\mathbf{R}_{\text{F0}})$, $J_{\text{Ca0}} = J_{\text{Ca}}(\mathbf{R}_{\text{F0}})$, $F_{\text{F}} = F_{\text{clus}}(\mathbf{R}_{\text{F}})$, and $F_{\text{Ca}} = F_{\text{clus}}(\mathbf{R}_{\text{Ca}})$. Note that one cannot write a force equation for the central F^- ion since by symmetry the net force on this ion is always zero and therefore does not represent an independent condition. Equations (19)–(22) represent the least complicated set of conditions to apply toward the solution of the parameters. These equations are linear in the q_{F} and q_{Ca} parameters and highly nonlinear in α_{F} and α_{Ca}. They cannot be solved analytically and may not even permit a numerical solution for certain values of the constants. The following numerical method always allows for at least an approximate numerical solution.

We first solve Eqs. (19) and (20) for the linear parameters q_{F} and q_{Ca},

$$\begin{aligned} q_{\text{F}} &= \frac{1}{A}(Z_{\text{Ca}} K_{\text{CaCa}} F_{\text{F}} - Z_{\text{F}} K_{\text{CaF}} F_{\text{Ca}}), \\ q_{\text{Ca}} &= \frac{1}{A}(-Z_{\text{Ca}} K_{\text{FCa}} F_{\text{F}} + Z_{\text{F}} K_{\text{FF}} F_{\text{Ca}}), \end{aligned} \tag{23}$$

where, $A = Z_{\text{Ca}} K_{\text{CaCa}} Z_{\text{F}} K_{\text{FF}} - Z_{\text{F}} K_{\text{CaF}} Z_{\text{Ca}} K_{\text{FCa}}$. Substituting into Eq. (21) produces

$$\begin{aligned} &Z_{\text{Ca}} K_{\text{CaCa}} F_{\text{F}} J_{\text{F0}} - Z_{\text{F}} K_{\text{CaF}} F_{\text{Ca}} J_{\text{F0}} \\ &\quad + Z_{\text{F}} K_{\text{FF}} F_{\text{Ca}} J_{\text{Ca0}} - Z_{\text{Ca}} K_{\text{FCa}} F_{\text{F}} J_{\text{Ca0}} \\ &\quad = Z_{\text{Ca}} K_{\text{CaCa}} Z_{\text{F}} K_{\text{FF}} V_0 - Z_{\text{F}} K_{\text{CaF}} Z_{\text{Ca}} K_{\text{FCa}} V_0 \end{aligned} \tag{24}$$

which contains only the α_{F} and α_{Ca} parameters. The next step is to scan the parameter α_{F} using Eq. (24) to calculate corresponding values of α_{Ca}. Then for each ordered pair $(\alpha_{\text{F}}, \alpha_{\text{Ca}})$, the ratio $q_{\text{Ca}}/q_{\text{F}}$ is calculated from Eq. (23). The solution chosen is the one that best satisfies Eq. (22). Because the external lattice is taken to be finite, we found that Eq. (22) could not be strictly satisfied in conjunction with solutions of Eq. (24). The $q_{\text{Ca}}/q_{\text{F}}$ ratio is listed along with the other parameters for each iteration of the embedding process and serves as an indicator of the accuracy by which Eqs. (19)–(22) are solved. A perfect solution of these equations will produce a $q_{\text{Ca}}/q_{\text{F}}$ ratio equal to −2.

III. RESULTS

The basis set for these calculations were optimized for the isolated cluster in the ground state [13]. Table II shows the results leading to the stabilization of the nondefective cluster, $(\text{Ca}_4\text{F}_7)^{1+}$, in the singlet ground state. The column labeled $F_{\text{clus}}(\mathbf{R}_j)\hat{\mathbf{r}}$ lists the forces on the F-site and Ca-site nuclei calculated quantum mechanically at the Hartree–Fock level of theory, except for the last row where they are calculated at the CISD level. It is important to note that the forces in this column do not include the direct coulombic interactions between the cluster nuclei and the surrounding external classical charge distribution but arise only from the interactions among the other cluster nuclei and the Hartree–Fock electronic density. As presently written, GAUSSIAN 92 incorporates into the Fock operator the coulombic interactions between the external charge and the cluster electronic charge density only. Thus, the cluster nuclei experience the presence of the external charge distribution only indirectly through its affect on the cluster Hartree–Fock density. The direct coulombic interaction must be included separately. The next column lists the effective charges and Gaussian exponents characterizing the external charge distribution at the given itera-

TABLE II

Results of the Iterative Embedding Procedure Based on Successive SCF Force Calculations and External Lattice-Centered Gaussian Variations

	$F_{\text{clus}}(\mathbf{R}_j)\hat{\mathbf{r}}$ (au)		New Parameters (au)					$F_{\text{ext}}(\mathbf{R}_j)\hat{\mathbf{r}}$ (au)		$F_{\text{net}}(\mathbf{R}_j)\hat{\mathbf{r}}$ (au)	
Iter.	F-site	Ca-site	q_F	α_F	q_{Ca}	α_{Ca}	q_{Ca}/q_F	F-site	Ca-site	F-site	Ca-site
0	−0.0857	−0.2435			-isolated cluster-			0.0000	0.0000	−0.0857	−0.2435
1	−0.0010	−0.0902	−0.710	0.030	1.432	0.018	−2.017	0.0857	0.2435	0.0847	0.1533
2	−0.0096	−0.1037	−1.067	0.025	2.142	0.020	−2.007	0.0010	0.0902	−0.0086	−0.0136
3	−0.0088	−0.1024	−1.028	0.025	2.065	0.020	−2.009	0.0096	0.1037	0.0008	0.0013
4	−0.0089	−0.1026	−1.032	0.025	2.073	0.020	−2.009	0.0088	0.1024	−0.0001	−0.0001
5	−0.0089	−0.1026	−1.032	0.025	2.072	0.020	−2.008	0.0089	0.1026	0.0000	0.0000
CISD	−0.0048	−0.1024			-same as above-			-same as above-		0.0041	0.0002

Note. This is a summary of the results applied to the nondefective $(Ca_4F_7)^{+1}$ cluster in the singlet ground state.

tion. Also listed is the ratio q_{Ca}/q_F. This is followed by a column labeled $F_{\text{ext}}(\mathbf{R}_j)\hat{\mathbf{r}}$ indicating the forces on the F-site and Ca-site cluster nuclei resulting from the direct coulombic interaction with the classical external charge distribution. The column labeled $F_{\text{net}}(\mathbf{R}_j)\hat{\mathbf{r}}$ is the vector sum of $F_{\text{clus}}(\mathbf{R}_j)\hat{\mathbf{r}}$ and $F_{\text{ext}}(\mathbf{R}_j)\hat{\mathbf{r}}$. The goal is to minimize $F_{\text{net}}(\mathbf{R}_j)\hat{\mathbf{r}}$ by a variation of the embedding parameters q_F, α_F, q_{Ca}, α_{Ca}, together with Hartree–Fock force calculations.

Figure 4 shows the net force on the F-site and the Ca-site nuclei, as well as the ratio of q_{Ca} to q_F for iterations 1 through 5. For iteration 0 the cluster is in isolation with no external charge. For the isolated cluster the SCF force calculation produces a net inward force on both the F-site and the Ca-site nuclei. Next with the external lattice size chosen to best approximate the cluster-subtracted Madelung potentials as described in Section II.C, Eq. (24) is solved subject to the condition $q_{Ca}/q_F \approx -2$ for the embedding parameters so that the resulting external forces, $F_{\text{ext}}(\mathbf{R}_j)\hat{\mathbf{r}}$, exactly balance the cluster forces, $F_{\text{clus}}(\mathbf{R}_j)\hat{\mathbf{r}}$, of the previous iteration. A new Hartree–Fock force calculation is then performed to produce new cluster forces which are then added to the external forces yielding the net forces for iteration 1. This process is repeated and, as Table II shows, is rapidly convergent, giving acceptably small net forces by the third iteration. To test the effects of correlation, a CISD force calculaton was performed using the parameters of iteration 5. While the resulting CISD net forces did increase over the Hartree–Fock forces, overall we think that the forces which include correlation are still acceptably small, given the approximations involved in this embedding model.

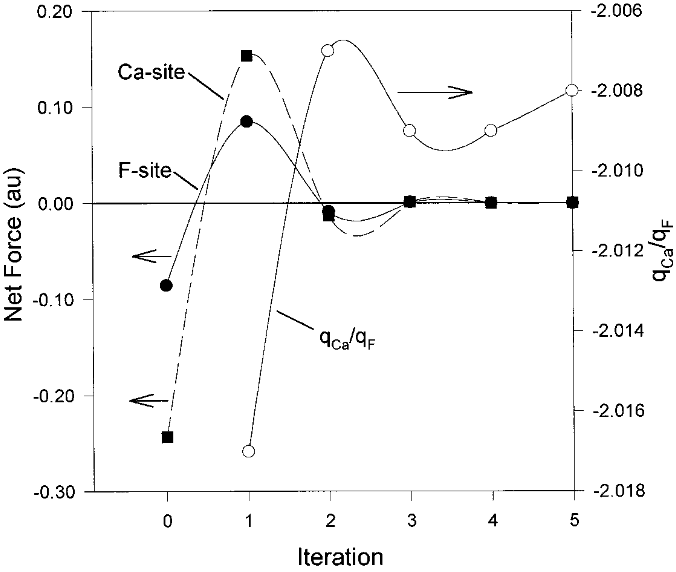

FIG. 4. The variation of the net forces on the F-site and Ca-site quantum cluster nuclei as well as the ratio q_{ca}/q_F for iterations 1 through 5. This is a graphical representation of some of the results presented in Table II.

With the nondefective cluster stabilized, the F-center cluster is then formed. Using the parameters from iteration 5 of Table II the central F^- ion is removed and an electron is added to the quantum cluster thereby forming the $(Ca_4F_6Vac)^{1+}$ $S = \frac{1}{2}$ F-center cluster. The geometry of this cluster is shown as Fig. 5. Modeling an electron in the vacancy involves the placement of basis functions in a region of space for which no nuclear core exists. Within the GAUSSIAN 92 set of programs this is accomplished by the use of "ghost atoms." A ghost atom is a location in space with zero nuclear charge, about which basis functions may be located. For our purpose, the ghost atom and the associated basis functions were used to model the electronic charge distribution within the vacancy [13]. The atomic basis functions were chosen to physically occupy most of the vacancy region with four *s*-type and six *p*-type uncontracted Gaussian functions centered at the origin.

The elimination of the central F^- ion will unbalance the

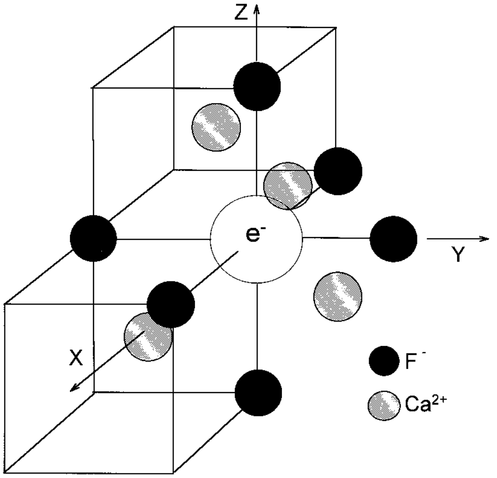

FIG. 5. Diagram of the F-center defect, $(Ca_4F_6Vac)^{1+}$, used to model the defect formed in CaF_2 following irradiation. After embedding and following relaxation, the vacancy-F and vacancy-Ca distances are 2.70 Å and 2.29 Å, respectively.

forces on the outer Ca^{2+} and F^- ions; hence the locations of these ions must be adjusted to new equilibrium positions. The parameters of iteration 5 of Table II are used to describe the external charge distribution and are held constant throughout the relaxation. After several inward adjustments of the Ca–Vac and F–Vac distances we obtained an order of magnitude decrease in the net forces on the ions. The final geometry was produced by a 1.2% inward relaxation for the F^- ions and a 3.3% inward relaxation for the nearest-neighbor Ca^{2-} ions. The magnitude and direction of these relaxations appear reasonable in view of recent calculations involving the relaxation of F-center defects in other ionic crystals by Vail and Woodward using the ICECAP program [14]. They describe an embedded F-center in NaF for which they find a 5% inward relaxation of the nearest-neighbor Na^+ ions.

IV. FINAL COMMENTS AND PRACTICAL IMPLICATIONS

In this article we present a cluster embedding method by which clusters of atoms, which are treated quantum mechanically, may be embedded in a classical distribution of charges represented by lattice-centered Gaussians. Since the classical source terms giving rise to the embedding electrostatic field enter into the formalism through the Fock operator, the Hartree–Fock orbitals generated by the SCF procedure automatically include distortions arising from the external field. While we have illustrated this embedding method by calculating forces on the cluster ions using Hartree–Fock wave functions obtained for each iteration, if one had the appropriate computer resources one could perform the embedding iterations using a correlated method such as CISD. In any event, since the final embedded orbitals form the basis for correlated methods such as the ground and the excited state CI or CASSCF, this embedding method is ideal for correlated embedded cluster calculations, including those which seek to determine many-electron ground and excited state energies (such as CASSCF).

A. *The Question of Electronic Equivalence*

Figure 4 shows that by the fifth iteration the net forces on the cluster ions have converged to zero and that the ratio of q_{Ca} to q_F is -2.008, indicating that an approximate simultaneous solution to Eqs. (19)–(22) has been achieved. However, while the net forces on the ions may be made negligible by this iterative process, this by itself will not ensure that sites of the same ion type will be electronically equivalent within the quantum cluster. Indeed, the fifth iteration Mulliken charges on the central and outer F^- ions are -0.658 au and -0.699 au, respectively. The reason for this difference stems from the fact that while the cluster ions are sitting in potential minima by the end of the embedding process, the values of these minima will in general not be the same at the central and outer F^- sites. By virtue of the fact that Eq. (21) is satisfied at each iteration, the external potential at the central F^- site is the cluster-subtracted Madlung potential, namely, -0.2328 hartree. However, the external potentials at the outer F^- and the Ca^{2+} sites are not constrained in this fashion so by the fifth iteration they are -0.2389 hartree and -0.2439 hartree, respectively (compare with column 2 of Table I).

Earlier attempts at developing a cluster embedding scheme involved the simultaneous solution to potential equations for the outer F^- and the Ca^{2+} sites, instead of the force equations (19) and (20) [15]. While convergence was obtained for this earlier method, and the external parameters were determined so as to reproduce the cluster-subtracted Madlung potential at all cluster sites, nonzero forces remained on the outer F^- and the Ca^{2+} ions. However, the final Mulliken charges on the central and outer F^- ions were in much better agreement. Thus, an all-potential embedding scheme produces better electronic equivalence between the central and outer F^- ions, but it unfortunately leads to nonzero net forces on the cluster ions. Consequently, this all-potential method was rejected for this study since the desired effect was to minimize the net forces for the nondefective cluster so that the geometry of the F-center could be determined by relaxing the structure of the quantum cluster following the removal of the central F^- ion and the addition of an electron.

B. *Generalization of the Embedding Method*

Given the above considerations, it is clear that the next logical step is to generalize this method in a way so as to produce an external electrostatic field at each iteration that not only produces forces on the cluster nuclei that balances the SCF forces but also reproduces as closely as possible the cluster-subtracted Madlung potentials everywhere within the quantum cluster region. In other words, Eq. (21) must be generalized. We will now briefly describe one way of generalizing the embedding technique presented in this paper.

If $V_{\mathrm{ext}}(\mathbf{R}_j)$ is the external potential on a three-dimensional grid of points $\mathbf{R}_j$ within the quantum cluster region (not necessarily nuclear sites) arising from an external charge distribution characterized by the parameters q_{F}, α_{F}, q_{Ca}, α_{Ca}, then this external potential is given by Eq. (17).

Thus if $V_{\mathrm{csmp}}(\mathbf{R}_j)$ is the known cluster-subtracted Madlung potential at $\mathbf{R}_j$, then for each iteration one seeks to minimize the least-squares function,

$$\sum_j [V_{\mathrm{csmp}}(\mathbf{R}_j) - q_{\mathrm{F}} J_{\mathrm{F}}(\mathbf{R}_j) + q_{\mathrm{Ca}} J_{\mathrm{Ca}}(\mathbf{R}_j)]^2 = \chi^2(\alpha_{\mathrm{F}}, \alpha_{\mathrm{Ca}}), \tag{25}$$

where $\mathbf{R}_j$ now locates *all* points within the quantum cluster. This function can be minimized while simultaneously satisfying the force Eqs. (19) and (20) by substituting Eq. (23) for q_{F} and q_{Ca}, thus making χ^2 a function only of α_{F} and α_{Ca}. Thus for each embedding iteration, the lattice parameters α_{F} and α_{Ca} would be determined by minimizing χ^2 by a nonlinear least-squares procedure. The iterations would be continued until both the net forces on the cluster ions and χ^2 become negligible. Aside from the problems inherent in nonlinear least-squares fitting (such as local minima, or the presence of singularities), the above generalized procedure is significantly more complicated and may not converge. In fact, lack of convergence will most certainly arise if the number of parameters and the degrees of freedom connected with the description of the external lattice are insufficient to satisfy all the desired conditions.

Another area where this method could use refinement would be to model the Pauli repulsion that would be experienced by the cluster electrons with the surrounding lattice had the surrounding lattice also been treated quantum mechanically. It is unfortunate that GAUSSIAN 92 does not have a feature that allows for the introduction of a repulsive term that would serve to enforce Pauli exclusion. However, we believe that such a repulsion could be modeled within the present scheme by placing at the external sites more than one Gaussian. A linear combination of several Gaussians could be used to fit the core density obtained from free atom calculations. Additional, more diffuse, Gaussians would model the valence density. During the iterations only the valence Gaussians would be varied. We note that we would be fitting core densities which would subsequently act as source terms in the Fock operator during the embedded SCF calculation. We distinguish this approach from that of Martin and Hay [10] who fit free-ion core potentials and do not iterate. This represents a needed extension of this method but it would not, in any essential way, change the basic numerical procedure outlined in this article. Only the number and type of Gaussians would increase. We also note that another method, recently discussed by Vail and Rao [16], for incorporating cluster-embedding exchange appears to be more general, but it is also more complicated and does not as easily lend itself for use with GAUSSIAN 92.

A few additional minor points should be considered that would further improve this technique. It is well known that the single-determinant Hartree–Fock wave functions will not by themselves produce the experimental geometry of a cluster [12]. Since, by this method, the SCF wave functions are determined in conjunction with the external lattice parameters so as to force the cluster to be stable in the experimental geometry, this will lead to distortions in the electronic charge density. We note that the nondefective cluster in $\mathrm{CaF_2}$ is composed of all singlet closed-shell ions and thus the difference between the ground state SCF wave functions and those obtained by correlated methods should be minimal. Nevertheless, an improvement could be realized if the final embedding iterations are performed at a higher level of quantum chemical theory such as CISD or MP4. Finally, we note that one could choose to reoptimize the basis in the presence of the external field just before the final embedding iterations. However, we note that this should be done with great care. Our preliminary results showed that when we attempt to reoptimize the basis that the basis functions become so extended that a significant portion of the quantum cluster charge actually leaves the cluster and accumulates around the external classical sites.

The type of external lattice described thus far is amongst the simplest of cases, namely, consisting of single Gaussians located at the two types of external sites in the $\mathrm{CaF_2}$ lattice. While such a system may be ill-suited for describing the polarization effects on the external lattice ions in the presence of a charged lattice defect such as the $\mathrm{F^+}$ center in the alkaline earth oxides, our results for the F-center and the Mn-perturbed F-center clusters in $\mathrm{CaF_2}$ show that this SCF embedding method works quite well despite its obvious limitations and it represents a significant improvement over the use of a truncated point ion lattice [17].

ACKNOWLEDGMENTS

We thank Konrad Brandermuhl at the Oklahoma State University Computer Center for his generous assistance. This work was funded in part by the Naval Surface Warfare Center under Contract No. N60921-89-Q-10-137 and by a grant from the U.S. Dept. of Education, No. P-200-A-900-59.

REFERENCES

1. M. J. Frisch, G. W. Trucks, M. Head-Gordon, P. M. W. Gill, M. W. Wong, J. B. Foresman, B. G. Johnson, H. B. Schlegel, M. A. Robb, E. S. Replogle, R. Gomperts, J. L. Andres, K. Raghavachari, J. S. Binkley, C. Gonzalez, R. L. Martin, D. J. Fox, D. J. Defrees, J. Baker, J. J. P. Stewart, and J. A. Pople, GAUSSIAN 92 (Gaussian Inc. Pittsburgh, PA, 1992).
2. G. G. Hall and C. M. Smith, *Int. J. Quantum Chem.* **25,** 881 (1984).
3. C. M. Smith and G. G. Hall, *Theor. Chim. Acta* **69,** 63 (1986).
4. J. H. Harding, A. H. Harker, P. B. Keegstra, R. Pandey, J. M. Vail, and C. Woodward, *Physica B*+C **131,** 151 (1985).
5. A. B. Kunz and J. M. Vail, *Phys. Rev. B* **38**(2), 1058 (1988); A. B. Kunz, J. Meng, and J. M. Vail, *ibid.* **38**(2), 1064 (1988).
6. B. G. Dick Jr. and A. W. Overhauser, *Phys. Rev.* **112,** 90 (1958).
7. J. M. Vail, *J. Phys. Chem. Solids* **51**(7), 589 (1990).
8. J. M. Vail, R. Pandey, and A. B. Kunz, *Rev. Solid State Sci.* **5,** 241 (1991).
9. N. W. Winter, R. M. Pitzer, and D. K. Temple, *J. Chem. Phys.* **86,** 3549 (1987).
10. R. L. Martin and P. J. Hay, *J. Chem. Phys.* **98,** 8680 (1993).
11. W. Hayes (Ed.), *Crystals with the Fluorite Structure* (Oxford Univ. Press, Oxford, 1974).
12. A. Szabo and N. S. Ostlund, *Modern Quantum Chemistry* (McGraw–Hill, New York, 1989).
13. A. C. Lewandowski and T. M. Wilson, *Phys. Rev. B* **53**(1), 100 (1995).
14. J. M. Vail and C. Woodward, *J. Phys. C:* **21,** 3901 (1988).
15. A. C. Lewandowski and T. M. Wilson, *Int. J. Quantum Chem. Symp.* **26,** 673 (1992).
16. J. M. Vail and Rao, *Int. J. Quantum Chem.* **53,** 67 (1995).
17. F. Sim, C. R. A. Catlow, M. Dupuis, J. D. Watts, and E. C. Clementi, in *Supercomputer Research in Chemistry and Chemical Engineering,* edited by K. F. Jensen and D. G. Truhlar, ACS Symposium Series No. 353 (American Chemical Society, Washington, DC, 1987).